IEEE Access
Multidisciplinary | Rapid Review | Open Access Journal

Received February 27, 2017, accepted April 17, 2017, date of publication April 24, 2017, date of current version May 17, 2017.

Digital Object Identifier 10.1109/ACCESS.2017.2696034

Outage Performance of the Full-Duplex Two-Way DF Relay System Under Imperfect CSI

CHENG LI[1], HAOYANG WANG[1], YAO YAO[2], ZHIYONG CHEN[1], (Member, IEEE), XIAOFAN LI[3], (Member, IEEE), AND SHA ZHANG[3]

[1]Department of Electrical Engineering, Shanghai Jiao Tong University, Shanghai 200240, China
[2]Huawei Technologies Co., Ltd., Shanghai 201206, China
[3]Shenzhen Institute of Radio Testing & Tech, Shenzhen 518000, China

Corresponding author: Yao Yao (yyao@eee.hku.hk)

This work was supported in part by the National Nature Science Foundation of China under Grant 61531009 and in part by the National High Technology Research and Development Program of China under Grant 863 5G 2014AA01A704.

ABSTRACT Contrary to the most existing works about the full-duplex (FD) relaying with perfect channel state information (CSI), this paper studies the outage performance of the two-way FD decode-and-forward relay network under the joint effects of the residual self-interference and imperfect CSI. We first derive the exact closed-form expressions of the system outage probability, based on which we obtain the outage probability under the perfect self-interference cancellation to investigate the impacts of the imperfect CSI on the system performance. In addition, to gain more insights about the imperfect CSI, we analyze the optimal power allocation scheme and an optimal relay node placement strategy, which minimize the system outage probability. The results reveal that the imperfect CSI will only affect the optimal power allocation, and the optimal relay node placement is related to the power ratio between the user nodes. Finally, analytical evaluations are performed to verify the theoretical results, and Monte Carlo simulations guarantee the correctness of the analytical evaluations.

INDEX TERMS Full-duplex, imperfect CSI, outage performance, decode-and-forward, two-way relay.

I. INTRODUCTION

Relay-assisted communication is an effective way to facilitate the information exchange procedures between the cell-edge located users within the current forth generation (4G) wireless communications networks [1], [2]. Field measurements demonstrated that the relay stations can enhance the remote indoor received signal power and improve the average throughput, especially for the downlink traffic [3], [4]. Owing to the various advantages, the relay-assisted communication has been highlighted in the design of the evolving fifth generation (5G) wireless communications to deal with the thousand-folded throughput increase. In this context, the conventional relay-assisted communication, which works in the half-duplex (HD) mode, is not sufficient due to the low spectrum utilization. Recently, the full-duplex (FD) mode, which can transmit and receive signals simultaneously within a common frequency band, has been proposed [5]. Intuitively, by removing the orthogonality limitation, the FD mode has the potentials to double the spectral efficiency of the HD mode. Practical implementations have showed that the FD mode has achieved a spectral efficiency gain of 1.87× over the standard HD mode [6], [7]. Therefore, to meet the goal of the 5G wireless network, the relay-assisted communications based on the FD mode have received great interest.

A. BACKGROUND AND MOTIVATION

The researches of the relay systems can date back to the 1970s when Van Der Meulen first introduced the three-node relay channel in [8], and in [9] the relay channel was also studied by Sato in terms of the capacity bound. However, the capacity bound were obtained under the relatively degenerate channels. Then in [10], the authors studied the capacity theorems of the degraded relay channel in the Gaussian case. The relay networks can be classified into two categories: one-way relaying or two way relaying.

One-way relaying means that the passages are delivered in only one direction, i.e., from the source to the destination [11]–[15]. Specifically, in [11], the authors have studied the cooperative diversity of the amplify-and-forward (AF) and decode-and-forward (DF) when the user nodes acted as relay node, and the outage performance was also investigated for the high signal-to-noise ratio (SNR). In [12], [13], the authors have analyzed the user cooperation systems from the information-theoretical aspect in terms of the achievable

region, outage probability and the cellular coverage. Specific user cooperative strategies was also proposed for the conventional code-division multiple access (CDMA) systems. Then in [14], the authors have investigated the cooperative diversity for the selective relaying where one of multiple user nodes is selected as the relay node, and the results showed that the full spatial diversity can be achieved by the space-time-coded protocol. However, all the papers have considered the perfect channel state information (CSI). In practical, due the the frequency selective channel, deep fading or Gaussian noises, the estimated CSI is usually different from the actual value when the signals are transmitted. In [16], the authors have studied the AF relay networks under imperfect source-to-relay CSI. The specific CSI requirements were also obtained under certain symbol error rate (SER). On the other hand, the one-way relaying has been challenged for the deficiency of the spectral using [15] since four time slots are needed to complete one information exchange procedure.

To improve the spectral efficiency, the three-phase time division broadcast (TDBC) [17] and the two-phase physical layer network coding (PNC) [18] or analog network coding (ANC) [19] for the two-way relaying has been developed [20]. Compared to the one-way approach, the three-phase TDBC relaying could achieve 33% spectral efficiency improvement [17]. However, for two-phase PNC relaying or ANC relaying, even 50% increasing of the spectral efficiency could be realized [20]. In [17], the system performances in terms of the outage probabilities of the TDBC and PNC relaying have been analyzed and compared. In [20], the outage performance was derived for the regime where the cell-edge users were interfered by the other co-channel users. However, the problem of the imperfect CSI has not been taken into account. In [21], the authors have studied the impacts of the imperfect CSI on the system performance in terms of the outage probability and ergodic rate of the two-way PNC relaying. In addition, in [22], the authors have studied the outage performance of the two-way PNC relay systems under the imperfect CSI. The results in both papers showed that the system performance could be greatly degraded by the imperfect CSI.

In order to further recover the spectral efficiency loss incurred by the HD mode, the FD mode, which transmits and receives signals simultaneous at the same frequency band, has been proposed [7]. The system performance of the FD relaying has been comprehensively studied under the assumption of perfect CSI [23]–[26]. In [23] and [24], the outage probabilities of the FD two-way relay systems under single user environment and multi-user environment have been analyzed, respectively. In [25], the authors have comprehensively studied the outage probability and the achievable rate for the FD one-way and two-way relay systems with the ANC protocol and PNC protocol, and the tradeoffs between the outage probability and the achievable rate, one-way relaying and two-way relaying have been highlighted. Thereafter, the authors have analyzed the achievable rate and outage probability of the FD relay system under the 5G wireless networks, where the backhaul link between the relay node and the base station has been considered. However, there are limited literatures have studied the impacts of imperfect CSI on the FD relay systems. To cover the impacts of the imperfect CSI, in [27], the authors have analyzed the achievable rate for the FD two-way ANC relay networks, and in [28], the authors have derived the outage probabilities for the FD two-way ANC relay system, both under imperfect CSI condition. However, to the best of the author's knowledge, there has not any reported works about how the imperfect CSI affects the FD two-way PNC relay networks. The PNC relaying, which could achieve better system performance of the ANC relaying [25] due to the cancellation of the noise at the relay node, has been widely deployed for the relay and cooperative systems. Due to the significant detrimental impacts of the imperfect CSI, it is urgent to answer the question that how the imperfect CSI behaves under the FD two-way PNC relay network for the future wireless communications. In addition, the practical issue of the FD mode, i.e., the residual self-interference (RSI) after self-interference cancellation (SIC) also greatly limit the system performance. The joint effects of the imperfect CSI and RSI need to be studied as well for the implementation of FD two-way relay systems in future wireless communications.

B. CONTRIBUTION

In this paper, we consider the FD two-way PNC relay system, where two user nodes, node A and node B, exchange information via the relay node R in a two-way manner. We analyze the system performance in term of the outage probability, which measures the robustness of the transmission [11]. The imperfect CSI of the links between the node A, the node B and the relay node R are taken into account. In summary, the main contributions of this paper are listed as follows:

- We have investigated the outage performance of the two-way FD DF relay systems. Contrary to the previous work [23], in this paper, we have adopted the PNC protocol at the relay node. In addition, we have considered the RSI, which was modeled as Rayleigh rather than Gaussian distributed interference according to the practical characterization [29], [30], to better investigate the impacts of the RSI on the system performance. What's more, imperfect CSI incurred by the imperfect channel estimation has been taken into account.
- The exact closed-form system outage probability has been obtained. The cross effects, i.e., the imperfect CSI of one link would affect another link, have been observed during the analysis. Furthermore, we have examined the detrimental effects of the cross effects by numerical simulations. In order to highlight the detrimental effects of the imperfect CSI, we further analyze the outage probability under perfect SIC.
- To improve the system outage performance under the impacts of imperfect CSI, we obtained the optimal power allocation between the user nodes A and B as well as the optimal relay placement. The results show

that the power allocation is affected by the imperfect CSI, whereas the optimal relay placement is free from impacts of the imperfect CSI. Finally, all the theoretical results are validated by the simulations.

C. OUTLINE

The remainder of this paper is organized as follows: Section II describes the imperfect CSI model, RSI model and physical-layer signal model in detail. The outage performance, optimal power allocation and optimal relay node placement are analyzed in Section III. Numerical simulations are presented in Section IV to verify the theoretical results. Finally, conclusions are drawn in Section V.

II. SYSTEM MODEL

In this section, we will first elaborate on the channel mode, which includes the imperfect CSI model and the RSI model. Then, the specific physical-layer signal model is described. Fig. 1 depicts the system model, where two user node A and B intend to exchange information via the relay node R in a two-way manner. All the node are working in the FD mode, i.e., transmit and receive signals simultaneously. The PNC based on the DF protocol is adopted at the relay node to process the signals [18].

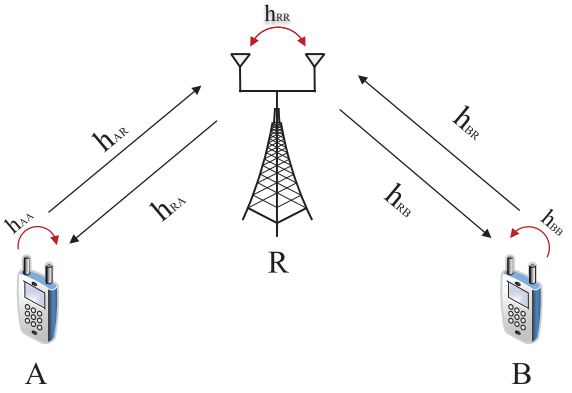

FIGURE 1. The FD two-way PNC relay system model, where the user node A and node B communicate with each other under the help of the relay node R.

A. CHANNEL MODEL

As Fig. 1 shows, we denote the channel coefficients of the link from the node A to node R and the versa link as h_{AR} and h_{RA}, respectively. Similarly, we denote the channel coefficients of the link from the node B to node R and the versa link as h_{BR} and h_{RB}, respectively. In this paper, we consider that all the channels are reciprocal, i.e., $h_{AR} = h_{RA}$ and $h_{BR} = h_{RB}$. In addition, we assume that the direct link between the node A and the node B does not exist due to large separation and strong shadowing effect. The messages can only be delivered by the relay node. Furthermore, for simplicity and without loss of generality, we assume that all the channels are subject to the block fading, i.e., the channel coefficients keep consistent within one time slot but changes independently over different time slots. Moreover, we assume the envelops of the channel coefficients are subject to the Rayleigh distribution. In order to take into account the effects of the RSI, we denote the self-interference channel at the user node A, the node B and the node R as h_{AA}, h_{BB} and h_{RR}, respectively.

1) IMPERFECT CSI MODEL

In this paper, we consider imperfect CSI incurred by the imperfect channel estimation of the links between the node A, the node B and the node R. We assume that the relay node adopts the minimum-mean-square-error (MMSE) method to estimate the channel coefficients [27], [28]. Thus, we can rewrite the channel model as

$$h_{AR} = \hat{h}_{AR} + \bar{h}_{AR}, \tag{1}$$

$$h_{BR} = \hat{h}_{BR} + \bar{h}_{BR}, \tag{2}$$

where h_{AR} and h_{BR} denote the actual value of the channel coefficients between node A and node R, node B and node R, respectively. $\hat{h}_{AR}$ and $\hat{h}_{BR}$ denote the estimated value of the channel coefficients between node A and node R, node B and node R, respectively. Accordingly, $\bar{h}_{AR}$ and $\bar{h}_{BR}$ denote the channel estimation errors of h_{AR} and h_{BR}, respectively. We assume that the envelopes of $\hat{h}_{AR}$ and $\hat{h}_{BR}$ are also subject to the Rayleigh distributions with $E\{|\hat{h}_{AR}|^2\} = \Omega_{\hat{h}_{AR}}$ and $E\{|\hat{h}_{BR}|^2\} = \Omega_{\hat{h}_{BR}}$, respectively. In addition, we assume that the channel estimation errors $\bar{h}_{AR}$ and $\bar{h}_{BR}$ are independent from $\hat{h}_{AR}$ and $\hat{h}_{BR}$, respectively. In addition, we assume that $\bar{h}_{AR}$ and $\bar{h}_{BR}$ are complex Gaussian random variables with zero mean and variances $\sigma^2_{\bar{h}_{AR}}$ and $\sigma^2_{\bar{h}_{BR}}$, respectively.

2) RSI MODEL

Besides the imperfect CSI, we also consider the imperfect SIC, which results in the RSI. According to the experimental characterization [29], the RSI channel exhibited Ricean distribution due to the line-of-sight component with a reduced K-factor. Thereafter, the results in [30] showed that by some passive SIC methods, the line-of-sight component can be greatly cancelled and the RSI channels were dominated by the reflected multipaths, which can be modeled as Rayleigh distribution. Hence, we denote the RSI channels at the user node A, the user node B and the relay node R as $\tilde{h}_{AA}$, $\tilde{h}_{BB}$ and $\tilde{h}_{RR}$, respectively, the envelop of which are subject to the Rayleigh distribution with the $E\{|\tilde{h}_{AA}|\} = \Omega_{\tilde{h}_{AA}}$, $E\{|\tilde{h}_{BB}|\} = \Omega_{\tilde{h}_{BB}}$ and $E\{|\tilde{h}_{RR}|\} = \Omega_{\tilde{h}_{RR}}$, respectively. The SIC capability for the node A and the node B can be denoted as $k_A = \lg(\Omega_{\tilde{h}_{AA}}/\Omega_{h_{AA}})$, $k_B = \lg(\Omega_{\tilde{h}_{BB}}/\Omega_{h_{BB}})$ and $k_R = \lg(\Omega_{\tilde{h}_{RR}}/\Omega_{h_{RR}})$, respectively.

B. PHYSICAL-LAYER SIGNAL MODEL

In this paper, we adopt the PNC based on the DF protocol at the relay node to process the signals. The signals at the relay node at the *n-th* time slot can be expressed as

$$y_R[n] = x_A[n]h_{AR}[n] + x_B[n]h_{BR}[n] + h_{RR}[n]x_R[n] + n_R[n], \tag{3}$$

TABLE 1. Transmitted signals in each time slot.

Time slot	1	2	···	n-1	n	···
Node A	$x_A[1]$	$x_A[2]$	···	x_A[n-1]	x_A[n]	···
Node B	$x_B[1]$	$x_B[2]$	···	x_B[n-1]	x_B[n]	···
Node R		$x_R[1]$	···	x_R[n-2]	x_R[n-1]	···

TABLE 2. Received signals in each time slot.

Time slot	1	2	···	n	n+1	···
Node A		$y_A[1]$	···	y_A[n-1]	y_A[n]	···
Node B		$y_B[1]$	···	y_B[n-1]	y_B[n]	···
Node R	$y_R[1]$	$y_R[2]$	···	y_R[n]	y_R[n+1]	···

where x_A, x_B and x_R denote the signals transmitted by the user node A and user node B with power P_A, P_B and P_R, respectively, $n_R[n]$ denotes the Gaussian noise with zero mean and variance σ_0^2. After SIC and using the CSI, the received signals at the relay node can be simplified as

$$y_R[n] = \hat{h}_{AR}[n]x_A[n] + \hat{h}_{BR}[n]x_B[n] + \bar{h}_{AR}x_A[n] + \bar{h}_{BR}[n]x_B[n] + \tilde{h}_{RR}y_R[n] + n_R[n] \quad (4)$$

Under the impacts of the imperfect CSI, the relay node jointly decodes the signals $x_A[n]$ and $x_B[n]$ and then perform the bit-level exclusive (XOR) operation of them and we denote the recoded signals as $x_R[n]$, i.e., $x_R[n] = x_A[n] \otimes x_B[n]$. Next, the relay node forward $x_R[n]$ to the node A and the node B with the power P_R. The received signals at the node A and node B after SIC can be expressed as

$$y_A[n] = \hat{h}_{AR}[n]x_R[n] + \bar{h}_{AR}x_R[n] + \tilde{h}_{AA}x_A[n] + n_A[n], \quad (5)$$

$$y_B[n] = \hat{h}_{BR}[n]x_R[n] + \bar{h}_{BR}x_R[n] + \tilde{h}_{BB}x_B[n] + n_B[n], \quad (6)$$

respectively, where $\tilde{h}_{AA}$ and $\tilde{h}_{BB}$ denotes the RSI channel incurred by the imperfect SIC, and $n_A[n]$ and $n_B[n]$ denote the Gaussian noise with zero mean and variance σ_0^2. After decoding $x_R[n]$ from the received signals, the user nodes A and B can perform the XOR operation of $x_R[n]$ with $x_A[n]$ and $x_R[n]$ with $x_B[n]$, respectively, to obtain the desired signals, i.e., $x_B[n] = x_R[n] \otimes x_A[n]$ for the node A and $x_A[n] = x_R[n] \otimes x_B[n]$ for the node B. For clarity, the transmitted signals and received signals in each time slot are summarized in the Table 1 and Table 2, respectively.

Hitherto, one information exchange process has been completed.

III. OUTAGE PERFORMANCE ANALYSIS

In this section, we first investigate the outage performance of the two-way FD PNC relay networks under the joint effects of the imperfect CSI and imperfect SIC. Then, we perform the asymptotic analysis, i.e., the user nodes could perfectly cancel the self-interference. Under the asymptotic scenario, we obtain the optimal power allocation scheme and the optimal relay location strategy.

Based on the physical-layer signal model, we can get the signal-to-interference-plus-noise ratio (SINR) as

$$\gamma_{AR} = \frac{|\hat{h}_{AR}|^2 P_A}{\sigma_{\tilde{h}_{AR}}^2 P_A + \sigma_{\tilde{h}_{BR}}^2 P_B + |\tilde{h}_{RR}|^2 P_R + \sigma_0^2}, \quad (7)$$

$$\gamma_{BR} = \frac{|\hat{h}_{BR}|^2 P_B}{\sigma_{\tilde{h}_{AR}}^2 P_A + \sigma_{\tilde{h}_{BR}}^2 P_B + |\tilde{h}_{RR}|^2 P_R + \sigma_0^2}, \quad (8)$$

$$\gamma_{RA} = \frac{|\hat{h}_{AR}|^2 P_R}{\sigma_{\tilde{h}_{AR}}^2 P_R + |\tilde{h}_{AA}|^2 P_A + \sigma_0^2}, \quad (9)$$

$$\gamma_{RB} = \frac{|\hat{h}_{BR}|^2 P_R}{\sigma_{\tilde{h}_{BR}}^2 P_R + |\tilde{h}_{BB}|^2 P_B + \sigma_0^2}, \quad (10)$$

$$\gamma_{SUM} = \frac{|\hat{h}_{AR}|^2 P_A + |\hat{h}_{BR}|^2 P_B}{\sigma_{\tilde{h}_{AR}}^2 P_A + \sigma_{\tilde{h}_{BR}}^2 P_B + |\tilde{h}_{RR}|^2 P_R + \sigma_0^2}, \quad (11)$$

where γ_{AR} and γ_{BR} denote the SINR of the links from A to R and B to R, respectively, γ_{RA} and γ_{RB} denote the SINR of the links from R to A and R to B, respectively, and γ_{SUM} denotes the sum SINR of the signals from the node A and node B to the node R.

Remark 1: From the expression of γ_{AR} and γ_{BR} we can note that the imperfect CSI of h_{AR} not only affects the link from the node A to the node R, but also contaminates the link from the node B to the node R. And at the same time, the imperfect CSI of h_{BR} not only affects the link from the node B to the node R but also disturbs the link from the node A to the node R.

A. EXACT OUTAGE PROBABILITY

Based on the above expressions of the SINR, next we derive the exact outage probability of the considered system. The outage probability can be defined as the probability that the rate of any link of the system falls below the predefined minimum threshold. Thus the system outage event occurs if

$$\log_2(1+\gamma_{AR}) < r_0 \quad \text{or} \quad \log_2(1+\gamma_{BR}) < r_0, \quad (12)$$

$$\log_2(1+\gamma_{RA}) < r_0 \quad \text{or} \quad \log_2(1+\gamma_{RB}) < r_0, \quad (13)$$

$$\log_2(1+\gamma_{SUM}) < 2r_0, \quad (14)$$

Then, we can obtain the outage region of the system as

$$\begin{cases} |\hat{h}_{AR}|^2 P_A < \max\{t_3 R_0,\ (t_1 + \frac{P_A^2}{P_R}|\tilde{h}_{AA}|^2) R_0\}, \\ |\hat{h}_{BR}|^2 P_B < \max\{t_3 R_0,\ (t_2 + \frac{P_B^2}{P_R}|\tilde{h}_{BB}|^2) R_0\}, \\ |\hat{h}_{AR}|^2 P_A + |\hat{h}_{BR}|^2 P_B < R_1 t_3, \end{cases} \quad (15)$$

where $R_0 = 2^{r_0} - 1, R_1 = 2^{2r_0} - 1; t_1 = \sigma_{\tilde{h}_{AR}}^2 P_A, t_2 = \sigma_{\tilde{h}_{BR}}^2 P_B$ and $t_3 = \sigma_{\tilde{h}_{AR}}^2 P_A + \sigma_{\tilde{h}_{BR}}^2 P_B$. In this paper, we consider that the system is dominant by the imperfect CSI and the RSI, thus, the Gaussian noises are neglected in the analysis. In addition, since the relay node, which are usually deployed in outer space, can achieve higher hardware complexity and is not limited by the size. Thus, the self-interference can

$$P_{out,1} = \begin{cases} \frac{\mu_1}{\mu_1-\mu_2} f(0,0,t_3,(1+R_0)t_3) + \frac{\mu_2}{\mu_2-\mu_1} f(0,0,(1+R_0)t_3,t_3), & (\mu_1 \neq \mu_2) \\ (1+\mu_1 t_3 R_0) f(0,0,(2+R_0)t_3,0), & (\mu_1 = \mu_2) \end{cases} \tag{17}$$

$$P_{out,2} = \begin{cases} \frac{\mu_1\mu_2}{(\mu_1-\mu_2+\nu_1-\nu_2)(\mu_2+\nu_2)} f(t_2,(t_1+R_0t_3),t_3,(1+R_0)t_3 \\ + \frac{\mu_1\mu_2}{(\mu_2-\mu_1+\nu_2-\nu_1)(\mu_1+\nu_1)} f((t_2+R_0t_3),t_1,(1+R_0)t_3,t_3), & (\mu_1 \neq \mu_2 \text{ or } \nu_1 \neq \nu_2) \\ \mu_1\mu_2 \left[\frac{1}{(\mu_1+\nu_1)^2} + \frac{R_0t_3}{\mu_1+\nu_1} \right] f((1+R_0)t_3,0,(1+R_0)t_3+t_1,t_2), & (\mu_1 = \mu_2 \text{ and } \nu_1 = \nu_2) \end{cases} \tag{18}$$

$$P_{out,3} = \begin{cases} \frac{\mu_1\mu_2}{(\mu_1+\nu_1-\mu_2)(\mu_1+\nu_1)} f(t_2+R_0t_3,0,(1+R_0)t_3,t_3) - \frac{\mu_1}{\mu_1+\nu_1-\mu_2} f(t_2,0,t_3,(1+R_0)t_3) & (\mu_1+\nu_1 \neq \mu_2) \\ -\frac{\mu_1}{\mu_2}(1+\mu_2 t_3 R_0) f(-t_1,0,0,(2+R_0)t_3), & (\mu_1+\nu_1 = \mu_2) \end{cases} \tag{19}$$

$$P_{out,4} = \begin{cases} \frac{\mu_1\mu_2}{(\mu_2+\nu_2-\mu_1)(\mu_2+\nu_2)} f(0,t_1+R_0t_3,t_3,(1+R_0)t_3) - \frac{\mu_2}{\mu_2+\nu_2-\mu_1} f(0,t_1,(1+R_0)t_3,t_3) & (\mu_2+\nu_2 \neq \mu_1) \\ -\frac{\mu_2}{\mu_1}(1+\mu_1 t_3 R_0) f(0,-t_2,(2+R_0)t_3,0) & (\mu_2+\nu_2 = \mu_1) \end{cases} \tag{20}$$

be more efficiently eliminated. As the experimental results showed for the larger equipments, the self-interference could be suppressed to the noise floor [7]. Therefore, it is reasonable to consider the perfect SIC at the relay node, i.e., the RSI as the relay node disappears. The system outage probability is given in the following theorem.

Theorem 1: The exact closed-form system outage probability under the joint effects of the imperfect CSI and the RSI can be expressed as

$$P_{out} = 1 - P_{out,1} - P_{out,2} - P_{out,3} - P_{out,4} \tag{16}$$

where $P_{out,1}$, $P_{out,2}$, $P_{out,3}$ and $P_{out,4}$ are expressed as (17), (18), (19) and (20) on the top of this page, and the function $f(a,b,c,d) = \exp(-\nu_1 a - \nu_2 b - \mu_1 c - \mu_2 d)$ where $\mu_1 = \frac{R_0}{P_A \Omega_{\tilde{h}_{AR}}}$, $\mu_2 = \frac{R_0}{P_B \Omega_{\tilde{h}_{BR}}}$, $\nu_1 = \frac{P_R}{P_A^2 \Omega_{\tilde{h}_{AA}}}$ and $\nu_2 = \frac{P_R}{P_B^2 \Omega_{\tilde{h}_{BB}}}$, respectively.

Proof: See Appendix A. ∎

B. OUTAGE PROBABILITY UNDER PERFECT SIC

In addition to the exact outage probability analysis, in this subsection, we analyze the system outage probability under the perfect SIC, i.e., $\Omega_{\tilde{h}_{AA}}$ and $\Omega_{\tilde{h}_{BB}}$ approach to 0. In this case, the system is only harassed by the imperfect CSI, which is inherently incurred by the time delay and Doppler effects of the user nodes.

Corollary 1: The system outage probability under perfect SIC can be expressed as

$$P_{out} = \begin{cases} 1 - \frac{\mu_1}{\mu_1-\mu_2} h(t_3,(1+R_0)t_3) - \frac{\mu_2}{\mu_2-\mu_1} h((1+R_0)t_3,t_3), & (\mu_1 \neq \mu_2) \\ 1 - (1+\mu_1 t_3 R_0) h((2+R_0)t_3,0), & (\mu_1 = \mu_2) \end{cases} \tag{21}$$

where $h(a,b) = \exp(-a\mu_1 - b\mu_2)$.

Proof: When the user nodes A and B can perfectly cancel the self-interference, the variances of the RSI channels will approach to zero, i.e., $\Omega_{\tilde{h}_{AA}} \to 0$ and $\Omega_{\tilde{h}_{BB}} \to 0$. Then we can note that ν_1 and ν_2 will approach to infinity, i.e., $\nu_1 \to +\infty$ and $\nu_2 \to +\infty$. Substituting ν_1 and ν_2, we can obtain the expressions of system outage probabilities under perfect SIC. ∎

Note that in this case, only the impacts of the imperfect CSI on the system performance are considered, thus, the cross effects of the imperfect CSI between the links from the node A to the node R and the node B to the node R can be revealed.

To gain more insights of the system outage probability, in the following we analyze the optimal power allocation and optimal relay placement which minimize the system outage probability.

Proposition 1: The optimal power allocation scheme when $P_A + P_B = P_T$ under the perfect SIC can be expressed as

$$\alpha_0 = \frac{\sigma_{\tilde{h}_{BR}}}{\sigma_{\tilde{h}_{AR}}} \sqrt{\frac{\Omega_{\hat{h}_{AR}}}{\Omega_{\hat{h}_{AR}}}} \tag{22}$$

where $\alpha = \frac{P_A}{P_B}$ and α_0 denotes the optimal value of α.

Proof: See Appendix B. ∎

Note that we obtain the optimal power allocation scheme under the asymmetrical case, i.e., $\nu_1 \neq \nu_2$. However, actually this is a general scheme that under the symmetrical case $\alpha = 1$, which is coincident with the obtained proposition.

In addition to the optimal power allocation, we analyze the optimal relay node placement under the perfect SIC as well. Since the channel variances are usually related to the link distances, the location of the relay node will also affect the system outage performance. Based on model of the distances and channel variances [31]–[33], we first normalize the dis-

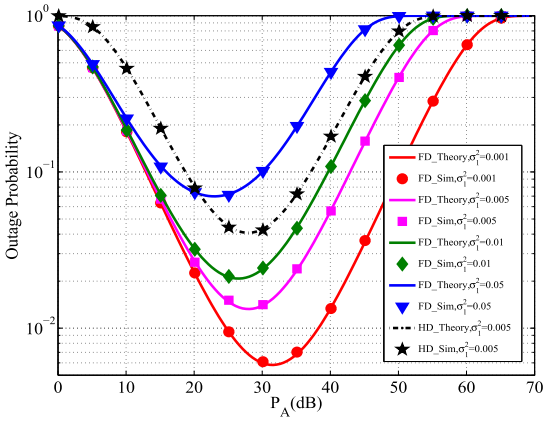

FIGURE 2. System outage probability vs. the transmit power P_A under different imperfect CSI cases.

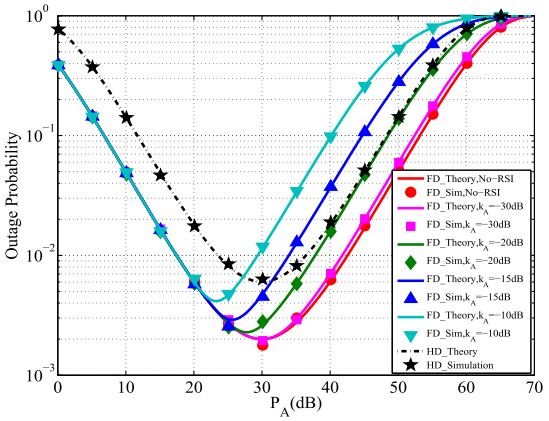

FIGURE 3. System outage probability vs. the transmit power P_A under different imperfect SIC cases.

tance of the link from $A \rightarrow R \rightarrow B$ to 1. Then, we use d and $1-d$, where $d \in (0,1)$, to denote the distance from the node A and the node B to the node R, respectively. Next, we model the channel variances of $\Omega_{\hat{h}_{AR}}$ and $\Omega_{\hat{h}_{BR}}$ inversely proportional to the d^{-4} and $(1-d)^{-4}$ [31]–[33]. The optimal relay placement are expressed in the following proposition.

Proposition 2: The optimal relay placement can be expressed as

$$d_0 = \frac{\alpha^{\frac{1}{3}}}{1+\alpha^{\frac{1}{3}}} \tag{23}$$

where d_0 denotes the optimal value of d and $\alpha = \frac{P_A}{P_B}$ is expressed in proposition 1.

Proof: See Appendix C. ■

Note that 1) the optimal d_0 is obtained via the asymmetrical case, however, it is actually a general optimal value which covers the symmetrical and asymmetrical both. 2) the optimal relay placement is only related to the transmit power. The reason is that the imperfect CSI has cross effects, i.e., the estimation error of the h_{AR} affects the link between B and R, and the estimation error of h_{BR} affects the link between A and R.

IV. NUMERICAL RESULTS

In this section, we conduct numerical simulations to verify the theoretical results. First, in Fig. 2 and Fig.3, we examine the relationship between the system outage probability and the transmit power of the user node A under different imperfect CSI cases and different RSI cases, respectively. The results of the HD counterparts are also presented for comparison. In the simulation, for clarity, we substitute $\sigma^2_{\hat{h}_{AR}}$ and $\sigma^2_{\hat{h}_{BR}}$ with σ_1^2 and σ_2^2, respectively.

In Fig.2, we plot the system outage probability with regard to P_A under four different imperfect CSI cases. In the simulation, we set the transmit power of the relay node R and the user node B as $P_R = 40$ dB, $P_B = 30$ dB, respectively, the SIC capability of the user nodes A and B as $k_A = k_B = -30$ dB, the minimum rate threshold as $r_0 = 1$ bps/Hz and the channel variances as $\Omega_{\hat{h}_{AR}} = 0.8$ and $\Omega_{\hat{h}_{AR}} = 1.2$, respectively. We note that under the same transmit power, the imperfect CSI will also deteriorate the outage performance, i.e., the higher σ_1^2, the greater the system outage probability. In addition, we note that imperfect CSI has greater impacts on the outage performance within high transmit power regime than low transmit power regime. Moreover, it is noted that the outage probability will first decrease and then increase with the transmit power and eventually approach to 1. The same situation goes as well even for the HD counterpart, which corroborates that it is the imperfect CSI that leads to the unavailability of the system. Hence, we obtain the insight that the imperfect CSI is critical for the high transmit power scenarios. The Monte Carlo simulations match the theoretical evaluations, which validates the correctness of the mathematical derivation.

In Fig. 3, we plot the system outage probability as a function of P_A under five different SIC cases. The variances of the channel estimation errors are set as $\sigma_1^2 = 0.005$ and $\sigma_2^2 = 0.005$ and the imperfect SIC capability of the node B is set as $k_B = -40$ dB. The other parameters are set as the same with that in Fig. 2. From the comparison of the FD mode and the HD mode, we obtain the insight that the FD mode can only improve the system performance within the low RSI regime. For example, when k_A is higher than -20 dB, the FD mode can hardly garner any performance gain over the HD mode. However, with high SIC capability, the FD mode can always achieve considerable performance gain compared the HD mode. In addition, we also note that the system outage probability will converge to 1 in the asymptotic transmit power scenarios, which indicates that the FD systems are transmit power sensitive systems.

Next, in order to investigate the relationship between the transmit power of the relay node P_R and the system outage probability, we plot the system outage probability in reference to P_R under different imperfect CSI cases and different imperfect SIC cases.

In Fig. 4, we investigate the impacts of the transmit power of the relay node P_R on the system outage performance under different imperfect CSI situations. In this figure, the transmit power of the user nodes A and B are set as $P_A = 30$ dB and

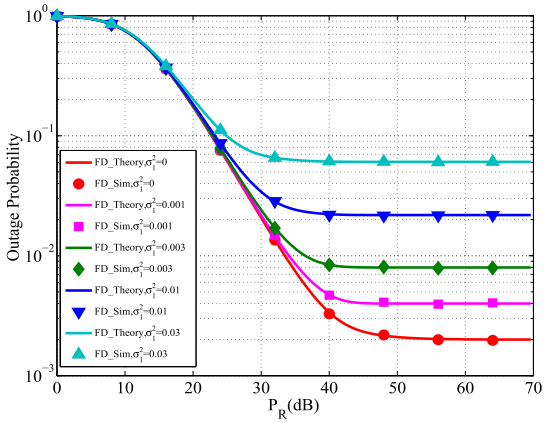

FIGURE 4. System outage probability vs. the transmit power P_R under different imperfect CSI cases.

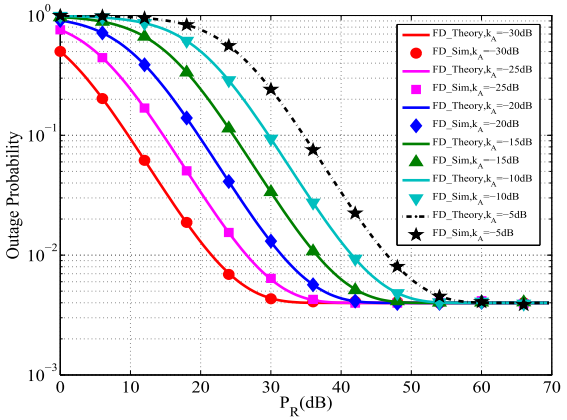

FIGURE 5. System outage probability vs. the transmit power P_R under different imperfect SIC cases.

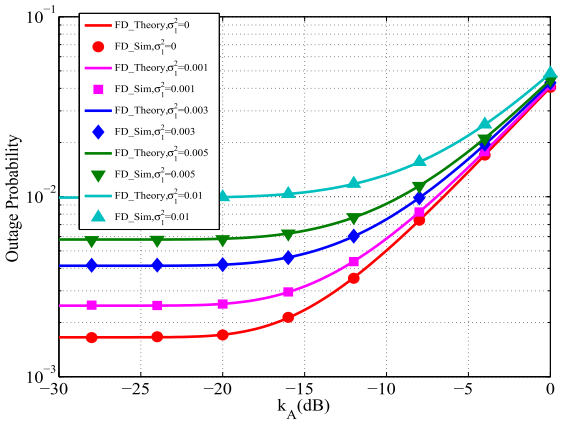

FIGURE 6. System outage probability vs. the SIC capability k_A under different imperfect CSI cases.

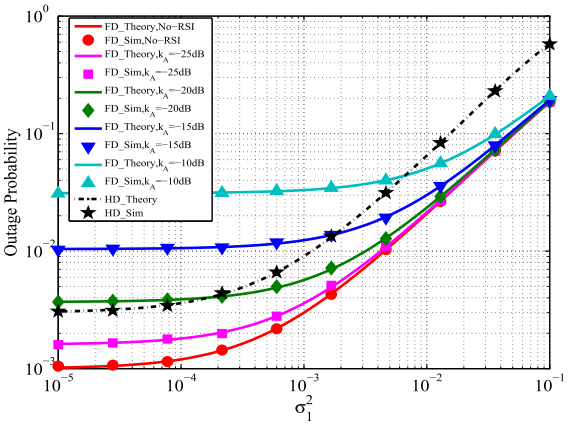

FIGURE 7. System outage probability vs. the imperfect CSI σ_1^2 under different imperfect SIC cases.

$P_B = 30$ dB, respectively. The SIC capability of the user node A and B are set as $k_A = -30$ dB and $k_B = -30$ dB. The channel variances are set as $\Omega_{\hat{h}_{AR}} = 0.8$ and $\Omega_{\hat{h}_{AR}} = 1.2$, the imperfect CSI $\sigma_2^2 = 0.01$ and the minimum rate threshold is set as $r_0 = 1$ bps/Hz. In this figure, we can note that the outage probability will decrease with the increase of P_R, and even under the asymptotic scenario, the outage probability will converge to the different minimum constant under different imperfect CSI rather than converge to 1. This reveal the insight that the transmit power of the system are less affected by the imperfect CSI even though under the same transmit power, the low quality of the CSI estimation will always lead to a higher outage probability.

In Fig. 5, we explore the impacts of the transmit power of the relay node P_R on the system outage probability under different SIC scenarios. In this figure, the variances of the imperfect CSI are set as $\sigma_1^2 = 0.01$ and $\sigma_2^2 = 0.01$, the channel variances $\Omega_{\hat{h}_{AR}} = 0.8$ and $\Omega_{\hat{h}_{AR}} = 1.2$ and other parameters are set as the same with the Fig. 4. In this figure, contrary to the figure 4, under different SIC capability, when P_R approach to infinity, all the cases will converge to a same minimum outage probability. However, under the low transmit power regime, SIC capability greatly affects the system outage probability. This phenomenon results from that the relay node can perfectly cancel the self-interference. It reveals the insight that under low transmit power regime of the relay node, the imperfect SIC of user nodes is critical to the system outage performance.

In order to observe the effects of the imperfect SIC and imperfect CSI on the system outage performance more directly, we plot the system outage probability as a function of the SIC capability of the user node A k_A and the imperfect CSI σ_1^2 in Fig. 6 and Fig. 7, respectively.

In Fig. 6, we simulate the system outage probability with relation to k_A under five different imperfect CSI cases. In this figure, the transmit power of the relay node and the user nodes A and B P_R are set to 35 dB, 30 dB and 30 dB. The imperfect CSI σ_2^2 is set to 0.002 and the imperfect SIC k_B is set to -40 dB. The minimum rate threshold is set to 0.5 bps/Hz and the channel variances are set as $\Omega_{\hat{h}_{AR}} = 1$ and $\Omega_{\hat{h}_{AR}} = 1$. In this figure, we can directly observe that the RSI greatly limits the system outage probability under the insufficient SIC capability. However, when the SIC exceeds a certain threshold, the system outage probability will converge to a

TABLE 3. Power allocation scheme.

Case	Exact Outage Region	β_a and β_2
A	$X < \alpha_1$ or $Y < \alpha_3$ or $X + Y < \alpha_5$	$\beta_1 \leq t_2R_0, \beta_2 \leq t_1R_0$
B	$X < \alpha_1$ or $Y < \alpha_4$ or $X + Y < \alpha_5$	$\beta_1 \leq t_2R_0, t_1R_0 < \beta_2 \leq t_3R_1 - t_3R_0 - t_2R_0$
C	$X < \alpha_1$ or $Y < \alpha_4$	$\beta_1 \leq t_2R_0, \beta_2 > t_3R_1 - t_3R_0 - t_2R_0$
D	$X < \alpha_2$ or $Y < \alpha_3$ or $X + Y < \alpha_5$	$t_2R_0 < \beta_1 \leq t_3R_1 - t_3R_0 - t_1R_0, \beta_2 \leq t_1R_0$
E	$X < \alpha_2$ or $Y < \alpha_3$	$\beta_1 > t_3R_1 - t_3R_0 - t_1R_0, \beta_2 \leq t_1R_0$
F	$X < \alpha_2$ or $Y < \alpha_4$ or $X + Y < \alpha_5$	$\beta_1 > t_2R_0, \beta_2 > t_1R_0, \beta_1 + \beta_2 \leq t_3R_1 - t_3R_0$
G	$X < \alpha_2$ or $Y < \alpha_4$	$\beta_1 > t_2R_0, \beta_2 > t_1R_0, \beta_1 + \beta_2 > t_3R_1 - t_3R_0$

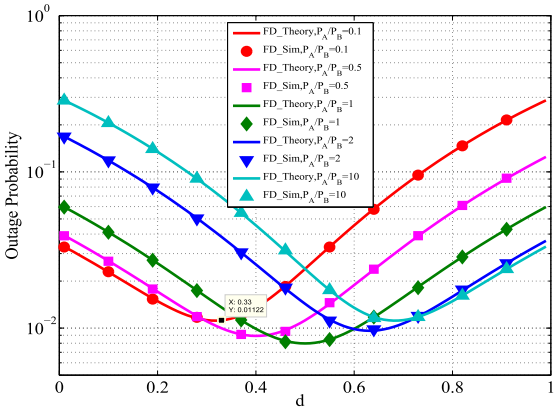

FIGURE 8. System outage probability vs. the relay placement.

constant, which reveals the insight the in the FD system, there is no need to perfectly cancel the self-interference at a high cost but to suppress the self-interference to a certain level.

In Fig. 7, we plot the system outage probability as a function of the imperfect SIC σ_1^2 under different SIC cases. In this simulation, the system parameters are set as that in figure 6. The outage probabilities of the HD counterparts are also presented. We can observe that the imperfect CSI will greatly limit the system performance. However, when σ_1^2 is less than 10^{-5} the system outage probability will converge to a constant, indicating that in the practical systems the imperfect CSI has to be alleviated to a certain level. In addition, it is noted that in the low imperfect CSI regime, the FD mode is superior to the HD mode only when the SIC capability exceeds a certain value. On the contrary, in the high imperfect CSI regime, the FD mode will superior to the HD mode no matter what level the SIC capability is.

In order to examine the impacts of the relay node placement on the system outage probability, in Fig. 8, we plot the system outage probability versus the relay node placement d. In this figure, the sum of the transmit power P_A and P_B is set to 33 dB, the transmit power of the relay node P_R is set to 45 dB, the imperfect CSI $\sigma_1^2 = 0.002$ and $\sigma_1^2 = 0.008$ and the minimum rate threshold is set to 1bps/Hz. By comparing the theoretical optimal value of d_0 and the simulated optimal value d_0, the optimal relay node placement strategy can be verified. For instance, when $P_A/P_B = 0.1$, the calculated optimal relay node placement is 0.32, which coincident with the simulated optimal value shown in the figure. When $P_A/P_B = 1$, it is easy to obtain that the optimal relay placement should be 0.5, meaning that the relay node should be placed in the center between the user node A and the user node B, which is also consistent with optimal relay placement in the figure.

V. CONCLUSION

In this paper, we studied the outage performance of the two-way FD relay system under the joint impacts of the imperfect CSI and imperfect SIC. We derived the exact system outage probability, based on which we obtained the outage probability under perfect SIC to study the cross effects of the imperfect CSI. Further more, the optimal power allocation scheme and optimal relay node placement strategy are proposed. By the simulations, we verified that the optimal relay placement does not relate to the imperfect CSI. In addition, the FD was superior to the HD mode whatever the RSI is under the high imperfect CSI regime. Finally, Monte Carlo simulations were performed to guarantee the correctness of the mathematical derivation.

APPENDIX A
PROOF OF THEOREM 1

From (15), we can observe that the specific region depends on the values of β_1 and β_2, where $\beta_1 = \frac{P_A^2}{P_R}|\tilde{h}_{AA}|^2R_0$ and $\beta_2 = \frac{P_B^2}{P_R}|\tilde{h}_{AA}|^2R_0$. Thus, the outage regions of different cases are expressed in the Table 3, where $X = |\hat{h}_{AR}|^2P_A$, $Y = |\hat{h}_{BR}|^2P_B$ and $\alpha_1 = t_3R_0$, $\alpha_2 = t_1R_0 + \beta_1$, $\alpha_3 = t_3R_0$, $\alpha_4 = t_2R_0 + \beta_2$ and $\alpha_5 = R_1t_3$. The outage probabilities corresponding to the different cases are expressed as

$$P_{out}^A = P_1(\alpha_1, \alpha_3) \quad (26)$$
$$P_{out}^B = P_1(\alpha_1, \alpha_4) \quad (27)$$
$$P_{out}^C = P_2(\alpha_1, \alpha_4) \quad (28)$$
$$P_{out}^D = P_1(\alpha_2, \alpha_3) \quad (29)$$
$$P_{out}^E = P_2(\alpha_2, \alpha_3) \quad (30)$$
$$P_{out}^F = P_1(\alpha_2, \alpha_4) \quad (31)$$
$$P_{out}^G = P_2(\alpha_2, \alpha_4) \quad (32)$$

where $P_1(x_1, x_2)$ is expressed as (24), as shown at the top of the next page, and $P_2(x_1, x_2)$ is expressed as

$$P_2(x_1, x_2) = 1 - e^{-\mu_1\frac{x_1}{R_0} - \mu_2\frac{x_2}{R_0}} \quad (33)$$

In this paper, we model the RSI channel as Rayleigh distributed with variances $\Omega_{\tilde{h}_{AA}}$ of the node A and $\Omega_{\tilde{h}_{BB}}$ of the

$$P_1 = \begin{cases} 1 - \dfrac{\mu_1}{\mu_1 - \mu_2} e^{(\mu_2-\mu_1)\dfrac{x_1}{R_0}} e^{-\mu_2(2+R_0)t_3} - \dfrac{\mu_2}{\mu_2 - \mu_1} e^{(\mu_1-\mu_2)\dfrac{x_2}{R_0}} e^{-\mu_1(2+R_0)t_3}, & \mu_1 \le \mu_2 \\ 1 - e^{-\dfrac{\mu_1 t_3 R_1}{R_0}} - \mu_1 \left(\dfrac{R_1 t_3 - x_1 - x_2}{R_0}\right) e^{-\mu_1(2+R_0)t_3}, & \mu_1 \le \mu_2 \end{cases} \tag{24}$$

$$\begin{aligned} P_{out} = & \int_0^{t_1 R_0} \int_0^{t_2 R_0} P_{out}^A f_{\beta_1}(x) f_{\beta_2}(y) dxdy + \int_{t_1 R_0}^{t_3 R_1 - t_3 R_0 - t_2 R_0} \int_0^{t_2 R_0} P_{out}^B f_{\beta_1}(x) f_{\beta_2}(y) dxdy \\ & + \int_{t_3 R_1 - t_3 R_0 - t_2 R_0}^{+\infty} \int_0^{t_2 R_0} P_{out}^C f_{\beta_1}(x) f_{\beta_2}(y) dxdy + \int_0^{t_1 R_0} \int_{t_2 R_0}^{t_3 R_1 - t_3 R_0 - t_1 R_0} P_{out}^D f_{\beta_1}(x) f_{\beta_2}(y) dxdy \\ & + \int_0^{t_1 R_0} \int_{t_3 R_1 - t_3 R_0 - t_1 R_0}^{+\infty} P_{out}^E f_{\beta_1}(x) f_{\beta_2}(y) dxdy + \int_{t_1 R_0}^{t_3 R_1 - t_3 R_0 - t_2 R_0} \int_{t_2 R_0}^{t_3 R_1 - t_3 R_0 - \beta_2} P_{out}^F f_{\beta_1}(x) f_{\beta_2}(y) dxdy \\ & + \int_{t_1 R_0}^{+\infty} \int_{t_2 R_0}^{+\infty} P_{out}^G f_{\beta_1}(x) f_{\beta_2}(y) dxdy - \int_{t_1 R_0}^{t_3 R_1 - t_3 R_0 - t_2 R_0} \int_{t_2 R_0}^{t_3 R_1 - t_3 R_0 - \beta_2} P_{out}^G f_{\beta_1}(x) f_{\beta_2}(y) dxdy \end{aligned} \tag{25}$$

node B, thus, the probability density function of β_1 and β_2 can be obtained as

$$f_{\beta_1}(x) = \lambda_1 e^{-\lambda_1 x} \tag{34}$$

$$f_{\beta_2}(x) = \lambda_2 e^{-\lambda_2 x} \tag{35}$$

where $\lambda_1 = \frac{P_R}{P_A^2 \Omega_{\hat{h}_{AA}}}$ and $\lambda_2 = \frac{P_R}{P_B^2 \Omega_{\hat{h}_{BB}}}$. Then the system outage probability can be expressed as (25), as shown at the top of this page.

Then by substituting (26), (34) and (35) into (25), the expression of P_{out} can be obtained as Theorem 1.

APPENDIX B
PROOF OF PROPOSITION 1

We assume that $P_T = P_A + P_B$ and use $\alpha = \frac{P_A}{P_B}$ to denote the transmit power ratio between the user nodes A and B. Substituting P_T andα into (21) and by using the Taylor expansion, we can rewrite the (21) as

$$\begin{aligned} P_{out} \approx & 1 - \frac{1}{1 - \dfrac{\Omega_{\hat{h}_{BR}}}{\Omega_{\hat{h}_{AR}}}\alpha} \left[1 - k\Omega_{\hat{h}_{AR}} - k(1+R_0)\Omega_{\hat{h}_{BR}}\alpha\right] \\ & - \frac{1}{1 - \dfrac{\Omega_{\hat{h}_{AR}}}{\Omega_{\hat{h}_{BR}}\alpha}} \left[1 - k(1+R_0)\Omega_{\hat{h}_{AR}} - k\Omega_{\hat{h}_{BR}}\alpha\right] \end{aligned} \tag{36}$$

where $k = R_0(\sigma^2_{\hat{h}_{AR}} + \frac{\bar{h}^2_{BR}}{\alpha})$, Then, by taking derivative with regard to α, we obtain that

$$\frac{\partial P_{out}}{\partial \alpha} = \frac{R_0}{P_T}[\sigma^2_{\hat{h}_{AR}} P_T \Omega_{\hat{h}_{AR}} - \frac{\sigma^2_{\hat{h}_{BR}} P_T \Omega_{\hat{h}_{BR}}}{\alpha^2}] \tag{37}$$

Then, by making $\frac{\partial P_{out}}{\partial \alpha}$ equal to 0, the optimal value of α can be obtained.

APPENDIX C
PROOF OF PROPOSITION 2

In order to obtain the optimal relay node placement, we model the channel variances proportional to the link distances. First, we normalize the link from the node A to the relay R and to the node B to 1. Then, we use d and $1-d$ to denote the distances from the nodes A and B to the relay node, respectively. According to [31]–[33], we model $\Omega_{\hat{h}_{AR}} = d^{-4}$ and $\Omega_{\hat{h}_{BR}} = (1-d)^{-4}$ and substitute them into (21). By using the Taylor series expansion and after some arithmetic operation, we can obtain that

$$\begin{aligned} P_{out} \approx & 1 - \frac{1}{1 - \dfrac{(1-d)^4}{d^4\alpha}} \left[1 - kd^4 - k(1+R_0)(1-d)^4\alpha\right] \\ & - \frac{1}{1 - \dfrac{d^4}{(1-d)^4\alpha}} \left[1 - k(1+R_0)d^4 - k(1-d)^4\alpha\right] \end{aligned} \tag{38}$$

where $k = R_0(\sigma^2_{\hat{h}_{AR}} + \frac{\bar{h}^2_{BR}}{\alpha})$, and then by taking derivative with regard to d we obtain

$$\frac{\partial P_{out}}{\partial d} = \frac{4k}{d^4 - (1-d)^4} \left[d^7 + \alpha^2(1-d)^7 - \alpha d^3(1-d)^3\right] \tag{39}$$

Then, by making $\frac{\partial P_{out}}{\partial d}$ to zero, the optimal relay node placement can be easily obtained.

REFERENCES

[1] C. Hoymann, W. Chen, J. Montojo, A. Golitschek, C. Koutsimanis, and X. Shen, "Relaying operation in 3GPP LTE: Challenges and solutions," *IEEE Commun. Mag.*, vol. 50, no. 2, pp. 156–162, Feb. 2012.

[2] B. Xia, C. Yang, and T. Cao, "Modeling and analysis for cache-enabled networks with dynamic traffic," *IEEE Commun. Lett.*, vol. 20, no. 12, pp. 2506–2509, Dec. 2016.

[3] J. Gan *et al.*, "LTE in-band relay prototype and field measurement," in *Proc. IEEE 75th Veh. Technol. Conf. (VTC Spring)*, May 2012, pp. 1–5.

[4] Y. Qian *et al.*, "Improving outdoor to indoor coverage by use of TD-LTE in-band relay," in *Proc. IEEE 24th Int. Symp. Pers. Indoor Mobile Radio Commun. (PIMRC)*, Sep. 2013, pp. 2658–2662.

[5] Z. Zhang, X. Chai, K. Long, A. V. Vasilakos, and L. Hanzo, "Full duplex techniques for 5G networks: Self-interference cancellation, protocol design, and relay selection," *IEEE Commun. Mag.*, vol. 53, no. 5, pp. 128–137, May 2015.

[6] M. Jain *et al.*, "Practical, real-time, full duplex wireless," in *Proc. ACM Int. Conf. Mobile Comput. Network.*, 2011, pp. 301–312.

[7] D. Bharadia, E. McMilin, and S. Katti, "Full duplex radios," *ACM SIGCOMM Comp. Commun. Rev.*, vol. 43, no. 4, pp. 375–386, 2013.
[8] E. C. Van Der Meulen, "Three-terminal communication channels," *Adv. Appl. Probab.*, vol. 3, no. 1, pp. 120–154, 1971.
[9] H. Satō, *Information Transmission Through a Channel With Relay*. Honolulu, HI, USA: Univ. Hawaii, 1976.
[10] T. M. Cover and A. A. El Gamal, "Capacity theorems for the relay channel," *IEEE Trans. Inf. Theory*, vol. 25, no. 5, pp. 572–584, Sep. 1979.
[11] J. N. Laneman, D. N. C. Tse, and G. W. Wornell, "Cooperative diversity in wireless networks: Efficient protocols and outage behavior," *IEEE Trans. Inf. Theory*, vol. 50, no. 12, pp. 3062–3080, Dec. 2004.
[12] A. Sendonaris, E. Erkip, and B. Aazhang, "User cooperation diversity. Part I. System description," *IEEE Trans. Commun.*, vol. 51, no. 11, pp. 1927–1938, Nov. 2003.
[13] A. Sendonaris, E. Erkip, and B. Aazhang, "User cooperation diversity. Part II. Implementation aspects and performance analysis," *IEEE Trans. Commun.*, vol. 51, no. 11, pp. 1939–1948, Nov. 2003.
[14] J. N. Laneman and G. W. Wornell, "Distributed space-time-coded protocols for exploiting cooperative diversity in wireless networks," *IEEE Trans. Inf. Theory*, vol. 49, no. 10, pp. 2415–2425, Oct. 2003.
[15] B. Rankov and A. Wittneben, "Spectral efficient protocols for half-duplex fading relay channels," *IEEE J. Sel. Areas Commun.*, vol. 25, no. 2, pp. 379–389, Feb. 2007.
[16] J. C. Lin, H. K. Chang, M. L. Ku, and H. V. Poor, "Impact of imperfect source-to-relay CSI in amplify-and-forward relay networks," *IEEE Trans. Veh. Technol.*, to be published, doi: 10.1109/TVT.2016.2622723.
[17] P. Liu and I. M. Kim, "Performance analysis of bidirectional communication protocols based on decode-and-forward relaying," *IEEE Trans. Commun.*, vol. 58, no. 9, pp. 2683–2696, Sep. 2010.
[18] R. H. Y. Louie, Y. Li, and B. Vucetic, "Practical physical layer network coding for two-way relay channels: Performance analysis and comparison," *IEEE Trans. Wireless Commun.*, vol. 9, no. 2, pp. 764–777, Feb. 2010.
[19] S. Katti, S. Gollakota, and D. Katabi, "Embracing wireless interference: Analog network coding," *ACM SIGCOMM Comput. Commun. Rev.*, vol. 37, pp. 397–408, Aug. 2007.
[20] X. Liang, S. Jin, X. Gao, and K. K. Wong, "Outage performance for decode-and-forward two-way relay network with multiple interferers and noisy relay," *IEEE Trans. Commun.*, vol. 61, no. 2, pp. 521–531, Feb. 2013.
[21] A. Hyadi, M. Benjillali, and M. S. Alouini, "Outage performance of decode-and-forward in two-way relaying with outdated CSI," *IEEE Trans. Veh. Technol.*, vol. 64, no. 12, pp. 5940–5947, Dec. 2015.
[22] S. Yadav and P. K. Upadhyay, "Impact of outdated channel estimates on opportunistic two-way ANC-based relaying with three-phase transmissions," *IEEE Trans. Veh. Technol.*, vol. 64, no. 12, pp. 5750–5766, Dec. 2015.
[23] C. Li, Z. Chen, Y. Wang, Y. Yao, and B. Xia, "Outage analysis of the full-duplex decode-and-forward two-way relay system," *IEEE Trans. Veh. Technol.*, to be published, doi: 10.1109/TVT.2016.2610004.
[24] B. Xia, C. Li, and Q. Jiang, "Outage performance analysis of multi-user selection for two-way full-duplex relay systems," *IEEE Commun. Lett.*, vol. 21, no. 4, pp. 933–936, Apr. 2017.
[25] Z. Zhang, Z. Ma, Z. Ding, M. Xiao, and G. K. Karagiannidis, "Full-duplex two-way and one-way relaying: Average rate, outage probability, and tradeoffs," *IEEE Trans. Wireless Commun.*, vol. 15, no. 6, pp. 3920–3933, Jun. 2016.
[26] Z. Zhang, Z. Ma, M. Xiao, G. K. Karagiannidis, Z. Ding, and P. Fan, "Two-timeslot two-way full-duplex relaying for 5G wireless communication networks," *IEEE Trans. Commun.*, vol. 64, no. 7, pp. 2873–2887, Jul. 2016.
[27] F. S. Tabataba, P. Sadeghi, C. Hucher, and M. R. Pakravan, "Impact of channel estimation errors and power allocation on analog network coding and routing in two-way relaying," *IEEE Trans. Veh. Technol.*, vol. 61, no. 7, pp. 3223–3239, Sep. 2012.
[28] D. Choi and J. H. Lee, "Outage probability of two-way full-duplex relaying with imperfect channel state information," *IEEE Commun. Lett.*, vol. 18, no. 6, pp. 933–936, Jun. 2014.
[29] M. Duarte *et al.*, "Design and characterization of a full-duplex multi-antenna system for WiFi networks," *IEEE Trans. Veh. Technol.*, vol. 63, no. 3, pp. 1160–1177, Mar. 2014.
[30] M. Duarte, C. Dick, and A. Sabharwal, "Experiment-driven characterization of full-duplex wireless systems," *IEEE Trans. Wireless Commun.*, vol. 11, no. 12, pp. 4296–4307, Dec. 2012.
[31] P. Liu and I.-M. Kim, "Performance analysis of bidirectional communication protocol based on decode-and-forward relaying," *IEEE Trans. Commun.*, vol. 58, no. 9, pp. 2683–2696, Sep. 2010.
[32] Z. Yi and I.-M. Kim, "An opportunistic-based protocol for bidirectional cooperative networks," *IEEE Trans. Wireless Commun.*, vol. 8, no. 9, pp. 4836–4847, Sep. 2009.
[33] T. S. Rappaport, *Wireless Communications: Principles and Practice*, vol. 2. Englewood Cliffs, NJ, USA: Prentice-Hall, 1996.

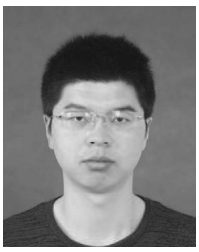

CHENG LI received the B.Eng. degree from the School of Electronics and Information, Northwestern Polytechnical University, Xi'an, China, in 2015. He is currently pursuing the Ph.D. degree with the Department of Electronic Engineering, Institute of Wireless Communications Technology, Shanghai Jiao Tong University, Shanghai, China. His research interests include full duplex antenna systems, cooperative communications, and resource allocation.

HAOYANG WANG is currently pursuing the B.S. degree with the Department of Electronic Engineering, Shanghai Jiao Tong University. His research interests include cooperative communications.

YAO YAO received the B.Eng. degree in computer science and the M.Eng. degree in circuits and systems from the University of Science and Technology of China, Hefei, China, in 1997 and 2000, respectively, and the Ph.D. degree in electrical engineering from The University of Hong Kong in 2004. Since 2005, she has been a Senior Research Scientist with Huawei Technologies Co., Ltd., on 3G wideband CDMA systems. Her research interests include synchronization and radio resource management.

ZHIYONG CHEN (S'08–M'12) received the B.S. degree in electrical engineering from Fuzhou University, Fuzhou, China, and the Ph.D. degree from the School of Information and Communication Engineering, Beijing University of Posts and Telecommunications, Beijing, China, in 2011. From 2009 to 2011, he was a Visiting Ph.D. Student with the Department of Electronic Engineering, University of Washington, Seattle, WA, USA. He is currently an Assistant Professor with the Cooperative Medianet Innovation Center, Shanghai Jiao Tong University, Shanghai, China. His research interests include mobile 3C networks, co-operative communications, physical-layer network coding, and 5G mobile communication systems. He serves as a TPC Member for major international conferences. He serves as the Publicity Chair of the IEEE ICCC 2014.

XIAOFAN LI (M'10) received the B.S. and Ph.D. degrees from the Beijing University of Posts and Telecommunication in 2007 and 2012, respectively. From 2010 to 2011, she was a Visiting Ph.D. Student with the University of Washington, Seattle, WA, USA. She has been involved in nearly ten national foundation projects. She is currently the Chief Engineer with the Shenzhen Institute of Radio Testing & Tech. Her research interests include radio equipment testing technology, cooperative transmission, cognitive radio, Internet of Things, and radio management policy.

SHA ZHANG received the B.S. and M.S. degrees from the Beijing University of Posts and Telecommunication in 2000 and 2004, respectively. He has participated over ten national level projects for broadband mobile communications and been awarded several times on the radio equipment automatic testing platform research and development by the China Institute of Communication Technological Progress. He is currently the Director of the Shenzhen Institute of Radio Testing & Tech. He is also the Chairman of Radio Spectrum and Electromagnetic Compatibility Work Group, Telematics Industry Application Alliance. His research interests include radio equipment testing technology and management field, radio spectrum management, intelligent transportation, and Internet of Things.